

Measuring the internal state of a single atom without energy exchange

Jürgen Volz¹, Roger Gehr¹, Guilhem Dubois^{1,2},
Jérôme Estève¹ & Jakob Reichel¹

¹Laboratoire Kastler-Brossel, ENS, CNRS, UPMC,
24 rue Lhomond, 75005 Paris, France.

²Present address: Astron FIAMM, 83210 La Farlède, France

May 17, 2011

Real quantum measurements almost always cause a much stronger back action than required by the laws of quantum mechanics. Quantum non-demolition (QND) measurements have been devised [1–6] such that the additional back action is kept entirely within observables other than the one being measured. However, this back action to other observables often also imposes constraints. In particular, free-space optical detection methods for single atoms and ions such as the shelving technique [7], though being among the most sensitive and well-developed detection methods in quantum physics, inevitably require spontaneous scattering, even in the dispersive regime [8]. This causes irreversible energy exchange and heating, a limitation for atom-based quantum information processing where it obviates straightforward reuse of the qubit. No such energy exchange is required by quantum mechanics [9]. Here we experimentally demonstrate optical detection of an atomic qubit with significantly less than one spontaneous scattering event. We measure transmission and reflection of an optical cavity [10–13] containing the atom. In addition to the qubit detection itself, we quantitatively measure how much spontaneous scattering has occurred. This allows us to relate the information gained to the amount of spontaneous emission, and we obtain a detection error below 10% while scattering less than 0.2 photons on average. Furthermore, we perform a quantum Zeno type experiment to quantify the measurement back action and find that every incident photon leads to an almost complete state collapse. Together, these results constitute a full experimental characterisation of a quantum measurement in the “energy exchange-free” regime below a single spontaneous emission event. Besides its fundamental

interest, this means significant simplification for proposed neutral-atom quantum computation schemes [14] and may enable sensitive detection of molecules and atoms lacking closed transitions.

In the first step of a measurement, the system to be measured becomes entangled with another quantum object (“meter”), such as a photon field. For the case of a two-level system (qubit), $(\alpha|0\rangle + \beta|1\rangle) \otimes |\Psi_{\text{in}}\rangle$ evolves into $\alpha|0\rangle \otimes |\Psi_0\rangle + \beta|1\rangle \otimes |\Psi_1\rangle$. The readout of the qubit then amounts to distinguishing the meter states $|\Psi_0\rangle$ and $|\Psi_1\rangle$, which can only be achieved up to some error because they are generally nonorthogonal. The minimum possible detection error $\epsilon = (\epsilon_0 + \epsilon_1)/2$ is given by the Helstrom bound [15]

$$\epsilon_H = \frac{1}{2} \left(1 - \sqrt{1 - |\langle \Psi_0 | \Psi_1 \rangle|^2} \right), \quad (1)$$

where ϵ_0 and ϵ_1 are the probabilities to measure the qubit in $|1\rangle$ although it was in $|0\rangle$ and vice versa and we assume no prior knowledge on the qubit state. In the following, we consider the generic case where a qubit is probed by an incident coherent light pulse containing n photons on average. To good approximation, the two final states $|\Psi_0\rangle$ and $|\Psi_1\rangle$ then also consist of coherent states. As an example, consider an ideal fluorescence measurement in which the dark state $|0\rangle$ does not interact with the light, while the bright state $|1\rangle$ scatters all photons. In this case, $|\Psi_0\rangle = |0\rangle_S |n\rangle_T$ and $|\Psi_1\rangle = |n\rangle_S |0\rangle_T$, where $|n\rangle$ is a coherent pulse containing n photons on average, and S and T refer to the scattered and transmitted light modes. Then, $|\langle \Psi_0 | \Psi_1 \rangle|^2 = \exp(-2n)$, and in the limit of large n one obtains $\epsilon_H \approx \exp(-2n)/4$. More generally, in all schemes using coherent pulses (so that $|\Psi_0\rangle$ and $|\Psi_1\rangle$ are tensor products of coherent states each containing a photon number proportional to n), $|\langle \Psi_0 | \Psi_1 \rangle|^2 = \exp(-\zeta n)$ with some real ζ . This exponential decrease of the minimum detection error with n naturally leads to a heuristic definition of the “knowledge” on the atomic state as $K \equiv -\ln 2\epsilon$. The maximum knowledge K_H one can obtain from a measurement is then $K_H = -\ln 2\epsilon_H$. We use the notation $f(x) = -\ln \left(1 - \sqrt{1 - \exp(-x)} \right)$, which for large x simplifies to $f(x) \approx x$. Thus, for coherent pulse schemes, $K_H = f(\zeta n)$ is the knowledge that the environment has obtained during the measurement, and constitutes an upper bound to the knowledge K_{acc} that the experimenter can actually access. In the case of the ideal fluorescence measurement, the maximum knowledge is $f(2n) \approx 2n$.

The measurement leads to a back action on the atom. The final state of the qubit after the measurement is obtained by tracing over the meter [16]: the coherence of the qubit is reduced, $\rho_{0,1} \rightarrow \langle \Psi_0 | \Psi_1 \rangle \rho_{0,1}$, where ρ is the qubit density matrix. This intrinsic back action need not affect other degrees of freedom (DOFs) of the system: DOFs which do not get entangled with the meter can be factored out and remain unaffected by the measurement. Most

real measurements, however, cause a much larger back action. In particular, fluorescence measurements are inevitably accompanied by spontaneous emission, which leads to heating and may pump the atom to an internal state outside the qubit basis. In the example of an ideal fluorescence detection, each incident photon is spontaneously scattered when the atom is in the bright state. Therefore, in terms of scattered photons m , the maximum knowledge can be expressed as

$$K_H = f(2m) \approx 2m. \quad (2)$$

This bound in fact applies to all free-space measurement methods in which classical light sources are used in a single-pass configuration [8]: in all such methods, information gain is necessarily accompanied by energy exchange between the atom and the light. In particular, this includes dispersive measurements with far off-resonant light. Moreover, even state-of-the-art experiments typically fall short of this limit by several orders of magnitude due to limited collection efficiency and require the scattering of a large number of photons to infer the qubit state. [17]

We overcome this limit by coupling the atomic qubit to a cavity in the strong-coupling regime $C = g^2/2\kappa\gamma \gg 1$, where g describes the coherent atom-cavity coupling and κ (γ) is the cavity (atomic) decay rate. The cavity is resonant to an optical transition of the $|1\rangle$ state, and probed by a resonant light pulse (Fig. 1 a). An atom in the non-resonant state $|0\rangle$ has negligible effect on the cavity and all photons from the incident mode are transmitted, $|\Psi_0\rangle = |0\rangle_R |n\rangle_T$. By contrast, an atom in $|1\rangle$ detunes the cavity by more than its linewidth, so that almost all photons are reflected, $|\Psi_1\rangle \approx |n\rangle_R |0\rangle_T$. The states $|\Psi_0\rangle$ and $|\Psi_1\rangle$ thus have the same overlap as in the ideal fluorescence measurement, and $K_H = f(2n)$ as before. Now, however, the atom sees a significant light intensity only when it is in the non-resonant state. Quantitatively, the $|1\rangle$ state only scatters a fraction $1/C$ of the incident photons [18, 19]. Therefore, the maximum knowledge per *scattered* photon is C times larger than the free-space limit:

$$K_H = f(2Cm) \approx 2Cm. \quad (3)$$

Furthermore, in contrast to fluorescence measurements, $|\Psi_0\rangle$ and $|\Psi_1\rangle$ are modes that are easily experimentally accessible. The atomic state can therefore be inferred with negligible spontaneous emission in a realistic experimental setup.

Our implementation of this cavity readout scheme is shown in Fig. 1 b. The key element is a fiber-based high-finesse cavity [20, 21] ($g = 2\pi 185 \pm 8$ MHz, $\kappa = 2\pi 53 \pm 0.5$ MHz, $\gamma = 2\pi 3$ MHz, $C = 108 \pm 8$) mounted on an atom chip. We prepare a Bose-Einstein condensate of ^{87}Rb atoms, from which we load a single atom into an intracavity dipole trap [22]. Levels and transitions are shown in Fig. 1 b. As shown earlier [22], cavity transmission

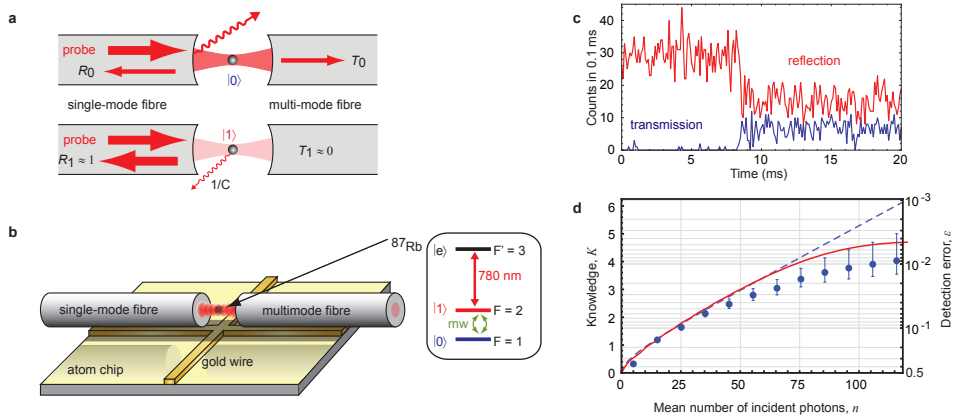


Figure 1: **Cavity-assisted detection of an atomic qubit.** **a**, For an atom in the dark state $|0\rangle$, probe light is either transmitted, reflected or lost by mirror imperfections. For the bright state $|1\rangle$, most incident photons are reflected. In both cases, only a small fraction is scattered by the atom. **b**, Our cavity is formed by the coated end facets of two optical fibres. The qubit states ($F = 1, m_F = 0$ and $F = 2, m_F = 0$) can be coupled by a resonant microwave. Cavity and the atomic transition $|1\rangle \rightarrow |e\rangle$ are resonant to the π -polarised probe laser at 780 nm. **c**, Typical detection trace showing cavity transmission (blue) and reflection (red) for an atom initially in $|1\rangle$ performing a quantum jump to $|0\rangle$ due to spontaneous emission. **d**, Detection error and corresponding knowledge on the atomic state with one s.d. error bars versus incident photon number n . The dashed line is the theoretical prediction taking into account our cavity imperfections (see text). We exclude the possibility of quantum jumps during the measurement which explains the deviation for large n . The solid line is the full simulation of our detection process including quantum jumps.

and reflection allow us to efficiently read out the atomic qubit state (see Fig. 1 c). Compared to the ideal situation described above, our system suffers from mirror losses and from the presence of the second TEM00 cavity mode with orthogonal polarisation detuned by 540 MHz, which has a non-negligible coupling to the atom (see methods). Losses reduce the empty-cavity transmission to $T_0 = 0.13$ with associated reflection $R_0 = 0.42$. The presence of the second mode together with the effect of the hyperfine atomic structure degrades the extinction ratio of the transmission when a resonant atom is present. Instead of the ratio $T_1/T_0 = 1/(4C^2)$ expected for a single-mode cavity coupled to a two-level atom, we measure $T_1/T_0 = 2\%$ (see Fig. 1 c), where $T_1 = 0.0024$ ($R_1 \approx 1$) is the cavity transmission (reflection) with an atom in the resonant state $|1\rangle$. The two field states $|\Psi_0\rangle$ and $|\Psi_1\rangle$ now have additional components for the loss channels and for the outgoing modes coupled to the second cavity mode. This increases $\langle \Psi_0 | \Psi_1 \rangle$, leading to a reduced $K_H = f(0.62n)$ (see methods). However, the intensity inside the cavity is also reduced by the mirror loss and therefore the expected

knowledge in terms of scattered photons is still much higher than m (see methods).

Knowledge on the atomic state carried by photons lost at the mirrors is not accessible to the experimenter, reducing the available knowledge to $f(0.23n)$. Furthermore, photon counting in the reflected and transmitted modes is not an optimal strategy to distinguish the two states $|\Psi_0\rangle$ and $|\Psi_1\rangle$. The associated detection error ϵ_d is given by the overlap of the two probability distributions of reflected and transmitted counts detected when the atom is in $|0\rangle$ or $|1\rangle$. As predicted by the Chernoff bound [23], it decreases exponentially for large n with a rate ξ , where ξ can be calculated from the reflection and transmission coefficients of the cavity and the efficiency of the photon detectors (see methods). Therefore, in the large- n limit, the knowledge that can be experimentally accessed $K_{\text{acc}} = -\ln 2\epsilon_d$ follows the function $f(x)$ introduced above, with $x = \xi n$. We numerically checked that $K_{\text{acc}} \approx f(\xi n)$ is also a valid approximation for small n . Taking into account finite photon detection efficiencies (47% in transmission, 31% in reflection), we expect our detection method to yield $K_{\text{acc}} = f(4.6 \times 10^{-2}n)$ (which would increase to $f(0.11n)$ using perfect detectors). To verify this prediction, we prepare the atom in either of the qubit states $|0\rangle$ and $|1\rangle$ and measure the corresponding detection errors [22]. For $n < 40$, the measurement is in good agreement with the prediction (figure 1 d). For larger n , nonresonant excitation leads to a small probability of depumping the qubit from its initial state during the measurement [22], thereby reducing the accessible knowledge in the experiment.

Although we only detect part of the incident photons and therefore of K_{H} , we can still quantify K_{H} by its back action. We perform the following quantum Zeno [24] experiment: An atom is prepared in state $|0\rangle$ or $|1\rangle$ (see methods) and a microwave π -pulse applied on the $|0\rangle \leftrightarrow |1\rangle$ resonance. During the π -pulse of duration τ , we apply detection light with a variable average photon number n . The incident light measures the atomic state and thereby prevents the Rabi oscillation, as shown in Fig. 2. We model this system as a coherently driven qubit undergoing on average \tilde{n} projective measurements that are randomly distributed over τ , and solve the corresponding Bloch equations (BEs). We include technical imperfections (preparation, detection and pulse errors) which limit the maximal (minimal) transfer probability to 0.95 (0.02). From the measured transfer efficiency (Fig. 2), we infer \tilde{n} for each mean number of incident photons n and, as expected, observe a linear relationship $\tilde{n} = (0.37 \pm 0.02)n$ (inset of Fig. 2). To see how the maximum knowledge K_{H} is related to \tilde{n} , we consider the evolution of the qubit in the absence of the microwave pulse. The BEs predict a reduction of coherence by $\exp(-\tilde{n})$, while the equivalent description introduced before (partial trace over the “meter”) predicts $\langle \Psi_1 | \Psi_0 \rangle$. Thus, $\langle \Psi_1 | \Psi_0 \rangle = \exp(-\tilde{n})$, and $K_{\text{H}} = f(2\tilde{n})$. The Zeno measurement therefore yields $K_{\text{H}} = f((0.74 \pm 0.04)n)$, in reasonable agreement with the value

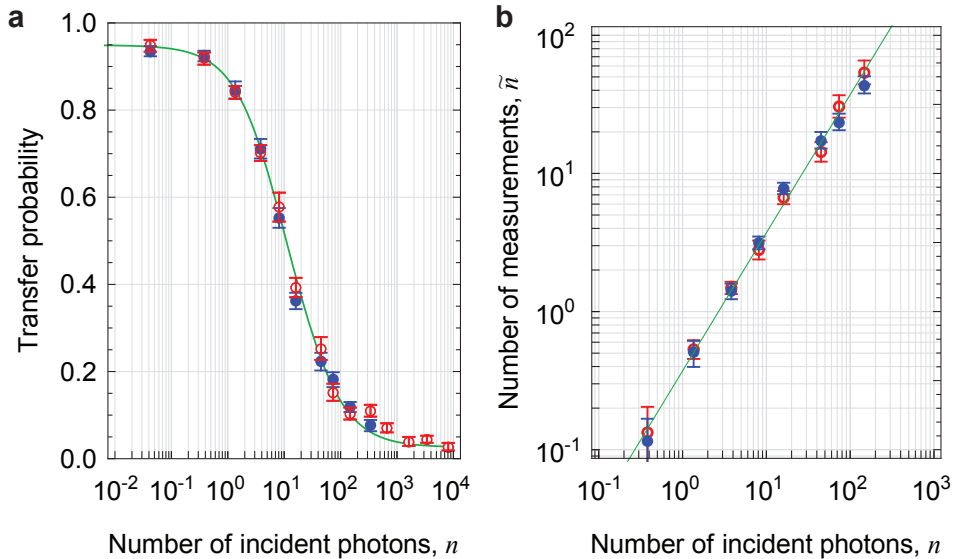


Figure 2: **Back action measurement using a quantum Zeno effect.** A microwave π -pulse (duration $8.8 \mu\text{s}$) is applied to an atom in $|1\rangle$ (\bullet) or $|0\rangle$ (\circ) in the presence of measurement light. **a**, Data points (with one s.d. error bars) show the transfer efficiency versus number of photons incident on the cavity during the pulse. **b**, The average number of projective measurements \tilde{n} we deduce for each data point from our model; the solid line is a linear fit $\tilde{n} = a_0 n$ yielding $a_0 = 0.37 \pm 0.02$. The solid line in **a** shows the prediction of our theoretical model supposing this linear relation and value of a_0 .

$K_H = f(0.62n)$ expected from photonic mode overlap. This shows that every single photon incident on the cavity leads to a significant state collapse, reducing the atomic coherence by a factor of 0.7.

In order to relate the maximum knowledge K_H and the accessible knowledge K_{acc} to the number of scattered photons m , we measure m as a function of n . Rather than attempting direct detection of the spontaneous photons (which would be inefficient and difficult to calibrate), we take advantage of the fact that each spontaneous scattering event of the $|1\rangle = |F=2, m=0\rangle$ state has a known probability to depump to other states $|F=2, m \neq 0\rangle$. The scattering rate of the off-resonant state $|0\rangle$ is three orders of magnitude smaller and can be neglected. We prepare the atom in $|1\rangle$ and turn on detection light for a variable time. Afterwards, we apply a microwave π -pulse on the $|1\rangle \leftrightarrow |0\rangle$ transition, and finally determine whether the atom has been transferred to $|0\rangle$. The microwave pulse has no effect on initial states $|F=2, m \neq 0\rangle$, so that its transfer probability to $|0\rangle$ is equal to the population remaining in $|1\rangle$ after the detection light pulse. We find that this survival probability decays exponentially with the number of incident photons with an initial rate $\nu = 1/(142 \pm 25)$ (Fig. 3). Because of the prob-

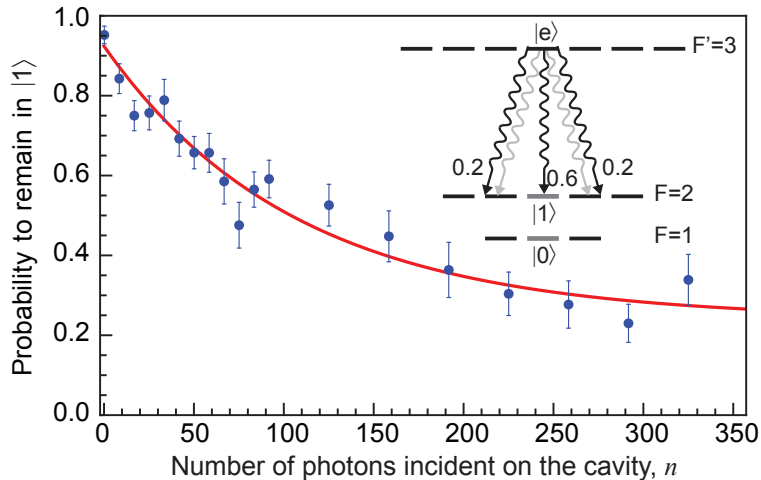


Figure 3: **Spontaneous emission during detection.** The datapoints (one s.d. error bars) show the measured probability that the atom remains in $|1\rangle$ during detection versus number of incident photons n . The solid line is a fit of an exponential decay to a steady-state population of 0.27 ± 0.05 with initial rate $\nu = 1/(142 \pm 25)$. The inset shows the two decay processes depleting $|1\rangle$. Detection light excites the state $|e\rangle$, which can decay into free space (black) with rate Γ or into the second cavity mode (light grey) with rate Γ_P (see methods). Correcting for decay back to $|1\rangle$ we obtain the number of scattered photons $m = n/(118 \pm 20)$.

ability to decay back to $|1\rangle$, the actual spontaneous emission rate is larger than this depumping rate. Correcting for this effect (see methods), we obtain $m/n = 1/(118 \pm 20)$. This is compatible with the theoretical prediction $m/n = 1/83$ for our particular atom-cavity system, where the second cavity mode increases the spontaneous emission rate (see methods). A still better value, $m/n = \sqrt{T_0}/C$, can be expected for a single-mode cavity.

We can now express K_H and K_{acc} in terms of scattered photons (figure 4). In the regime $m \ll 1$, where the detection efficiency is not limited by depumping, we find that our experiment extracts $K_H = f((87 \pm 17)m)$, of which $K_{\text{acc}} = f((5.4 \pm 0.9)m)$ is actually accessed. In spite of experimental imperfections, this knowledge gain is a factor of 2.7 higher than possible in an ideal fluorescence measurement and two orders of magnitude larger than in state-of-the-art experiments [17]. Since 118 photons on average can be sent onto the cavity before one scattering event occurs and each performs a strong measurement, a large amount of information on the atomic state can be obtained with negligible scattering. In this sense, one can say that the photons measure the atom without entering the cavity.

Note that our experiment is still limited by cavity imperfections that should be straightforward to improve. The closely spaced second cavity mode is a result of birefringence; experience with macroscopic cavities suggests that it can be either moved further away or made degenerate in future

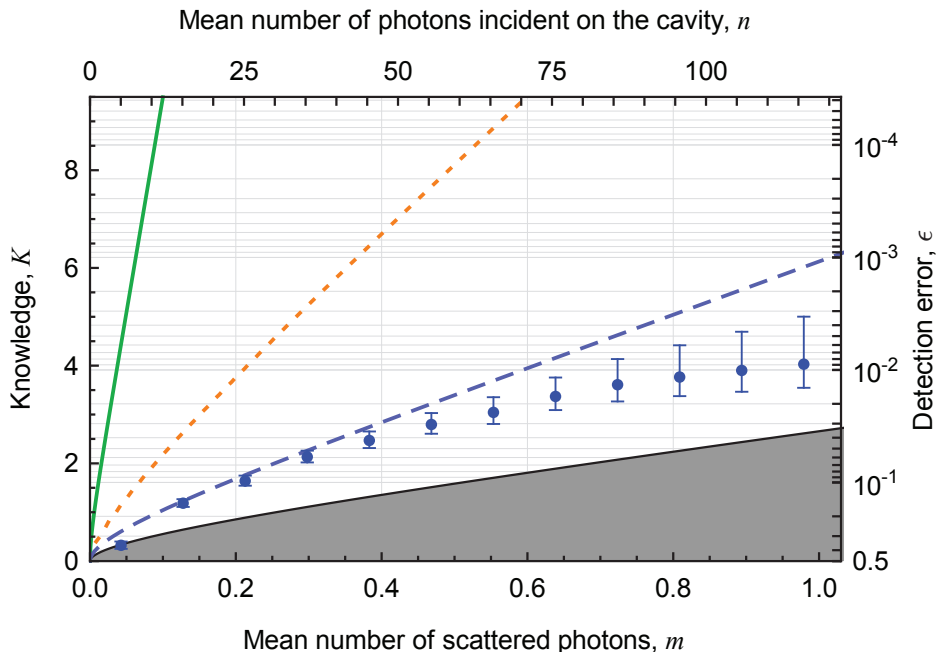


Figure 4: **Detection error and knowledge versus number of scattered photons.** The grey area is the range accessible to free-space detection schemes. This limit is overcome using a cavity. Green solid line: maximum knowledge K_H extracted by the cavity measurement, deduced from the data in figure 2. Orange dotted line: Accessible knowledge using our cavity with perfect photon counters to detect reflected and transmitted photons. Blue dashed line: accessible information K_{acc} with the detection efficiency in our experiment. Blue circles (\bullet): knowledge actually obtained from the experiment with one s.d. error bars. This knowledge is above the free-space limit in spite of experimental imperfections.

cavities. Cavity losses can be further reduced by at least a factor of four [21] by using state-of-the-art mirror coatings in an otherwise identical fiber cavity. Assuming these conditions and detector efficiencies of 70%, the accessible knowledge would be $K_{\text{acc}} \approx f(110m)$.

For our cavity parameters, heating mechanisms other than scattering are expected to be negligible [25]. Furthermore, the remaining scattering only leads to a small probability for the atom to change its vibrational state during detection, because of the Lamb-Dicke effect in our strong dipole trap. We estimate this probability to be two orders of magnitude smaller than in state-of-the-art fluorescence measurements for the same knowledge gain (in our case we can access $K_{\text{acc}} \approx 70$ before the creation of a phonon). This allows detection of atomic qubits while staying in the ground state of the trap, thereby removing the necessity of recoiling after read-out and drastically improving the cycling time of atom-based quantum computing schemes. Furthermore, the cavity readout scheme dispenses of the requirement for closed

transitions in state readout, opening perspectives for detection of single cold molecules [26].

References

- [1] Braginsky, V. B. & Khalili, F. Y. *Quantum Measurement* (Cambridge University Press, Cambridge, UK, 1992).
- [2] Grangier, P., Levenson, J. A. & Poizat, J.-P. Quantum non-demolition measurements in optics. *Nature* **396**, 537–542 (1998).
- [3] Nogues, G. *et al.* Seeing a photon without destroying it. *Nature* **400**, 239–242 (1999).
- [4] Maioli, P. *et al.* Nondestructive Rydberg Atom Counting with Mesoscopic Fields in a Cavity. *Phys. Rev. Lett.* **94**, 113601 (2005).
- [5] Hume, D. B., Rosenband, T. & Wineland, D. J. High-Fidelity Adaptive Qubit Detection through Repetitive Quantum Nondemolition Measurements. *Phys. Rev. Lett.* **99**, 120502 (2007).
- [6] Lupaşcu, A. *et al.* Quantum non-demolition measurement of a superconducting two-level system. *Nature Phys.* **3**, 119–125 (2007).
- [7] Leibfried, D., Blatt, R., Monroe, C. & Wineland, D. Quantum dynamics of single trapped ions. *Rev. Mod. Phys.* **75**, 281–324 (2003).
- [8] Hope, J. J. & Close, J. D. General limit to nondestructive optical detection of atoms. *Phys. Rev. A* **71**, 043822 (2005).
- [9] Kwiat, P., Weinfurter, H., Herzog, T., Zeilinger, A. & Kasevich, M. A. Interaction-Free Measurement. *Phys. Rev. Lett.* **74**, 4763–4766 (1995).
- [10] Boozer, A. D., Boca, A., Miller, R., Northup, T. E. & Kimble, H. J. Cooling to the Ground State of Axial Motion for One Atom Strongly Coupled to an Optical Cavity. *Phys. Rev. Lett.* **97**, 083602 (2006).
- [11] Puppe, T. *et al.* Trapping and Observing Single Atoms in a Blue-Detuned Intracavity Dipole Trap. *Phys. Rev. Lett.* **99**, 013002 (2007).
- [12] Khudaverdyan, M. *et al.* Quantum Jumps and Spin Dynamics of Interacting Atoms in a Strongly Coupled Atom-Cavity System. *Phys. Rev. Lett.* **103**, 123006 (2009).
- [13] Bochmann, J. *et al.* Lossless State Detection of Single Neutral Atoms. *Phys. Rev. Lett.* **104**, 203601 (2010).
- [14] Ladd, T. D. *et al.* Quantum Computers. *Nature* **464**, 45–53 (2010).
- [15] Helstrom, C. W. *Quantum detection and estimation theory*, vol. 123 of *Mathematics in Science and Engineering* (Academic Press, New York, 1976).
- [16] Haroche, S. & Raimond, J.-M. *Exploring the Quantum* (Oxford University Press, Oxford, 2006).
- [17] Gerber, S. *et al.* Quantum interference from remotely trapped ions. *New Journal of Physics* **11**, 013032 (2009).
- [18] Lugiato, L. A. Theory of optical bistability. In Wolf, E. (ed.) *Progress in Optics Vol. XXI*, 69–216 (Elsevier Science Publishers B.V., Amsterdam, 1984).
- [19] Hechenblaikner, G., Gangl, M., Horak, P. & Ritsch, H. Cooling an atom in a weakly driven high- Q cavity. *Phys. Rev. A* **58**, 3030–3042 (1998).
- [20] Colombe, Y. *et al.* Strong atom-field coupling for Bose-Einstein condensates in an optical cavity on a chip. *Nature* **450**, 272–276 (2007).

- [21] Hunger, D. *et al.* A fiber Fabry-Perot cavity with high finesse. *New J. Phys.* **12**, 065038 (2010).
- [22] Gehr, R. *et al.* Cavity-Based Single Atom Preparation and High-Fidelity Hyperfine State Readout. *Phys. Rev. Lett.* **104**, 203602 (2010).
- [23] Chernoff, H. A measure of asymptotic efficiency for tests of a hypothesis based on the sum of observations. *Ann. Math. Stat.* **23**, 493–507 (1952).
- [24] Itano, W. M. Perspectives on the quantum Zeno paradox. *arXiv:quant-ph/0612187v1* (2006).
- [25] Domokos, P. & Ritsch, H. Mechanical effects of light in optical resonators. *J. Opt. Soc. Am. B* **20**, 1098–1130 (2003).
- [26] Jones, K. M., Tiesinga, E., Lett, P. D. & Julienne, P. S. Ultracold photoassociation spectroscopy: Long-range molecules and atomic scattering. *Rev. Mod. Phys.* **78**, 483–535 (2006).

Acknowledgements This work was funded in part by the AQUITE Integrated Project of the EU (grant no. 247687), by the Institut Francilien pour la Recherche sur les Atomes Froids (IFRAF), and by the EURYI grant “Integrated Quantum Devices”.

Author contributions J.V., R.G. and G.D. performed the experiment. All authors contributed to data analysis and interpretation, as well as to the manuscript.

Author information The authors declare that they have no competing financial interests. Correspondence and requests for materials should be addressed to J. R. (email: jakob.reichel@ens.fr).

Methods

Preparation of the qubit states We initially extract a single atom in the $F=2$ hyperfine ground state and unknown Zeeman state from a BEC [22]. We then apply a microwave π -pulse on the qubit transition $|0\rangle \leftrightarrow |1\rangle$ followed by a short detection light pulse. If and only if the atom initially is in $|1\rangle$, the π -pulse transfers it to $|0\rangle$, leading to high cavity transmission. If it is in a different Zeeman sublevel, it remains in $F = 2$, leading to low transmission. In this case, spontaneous scattering due to the read out pulse leads to a redistribution in the $F = 2$ multiplet. We repeat the procedure until we detect high transmission, signaling an atom in $|0\rangle$. If we want to prepare the atom in $|1\rangle$ we apply an additional π -pulse.

Extracted and accessible knowledge from an imperfect cavity Assuming a coherent state with amplitude \sqrt{n} incident onto the cavity, a coherent field builds up in the cavity populating the main (resonant) and the orthogonally polarised, detuned TEM00 mode. Their amplitudes depend on the qubit state and each decays via three channels: transmission, reflection and losses at the mirrors. Thus the outgoing field can be approximated by the tensor product of six coherent fields with amplitudes $\alpha_i \sqrt{n}$. The subscript $i \in \{0, 1\}$ denotes the qubit state, while $\alpha \in \{t_m, r_m, l_m, t_d, r_d, l_d\}$ identifies the outgoing mode, m and d respectively designating the main and detuned mode. The overlap between the two possible light states $|\Psi_0\rangle$ and $|\Psi_1\rangle$ is then $\exp(-\zeta n)$ where $\zeta = \sum_{\alpha} |\alpha_0 - \alpha_1|^2$, leading to a maximum knowledge $f(\zeta n)$. In our case, the atom in state $|1\rangle$ is resonant to cavity and light field while the state $|0\rangle$ is far detuned. Under these circumstances the phase shift between the states $|\Psi_1\rangle$ and $|\Psi_0\rangle$ can be neglected and the amplitude coupling factors $\{\alpha_i\}$ can be considered real. The power coupling factors in percent are $\{\alpha_0^2\} = \{12.7, 41.4, 45.9, 0, 0, 0\}$ for an atom in $|0\rangle$ and $\{\alpha_1^2\} = \{0.1, 99, 0.4, 0.1, 0.1, 0.4\}$ for an atom in $|1\rangle$. From these values, we deduce $\zeta = 0.62$.

Using counters to detect the transmitted and reflected intensities, the detection error is minimised by using a maximum likelihood estimator (thresholding). The minimal error is $\epsilon_D = (1 - \|P_0 - P_1\|_1)/2$ where P_0 and P_1 are the probability distributions of detected counts if the qubit is in $|0\rangle$ or $|1\rangle$, and the distance $\|P_0 - P_1\|_1$ is defined as $\sum_{\mathbf{x}} |P_0(\mathbf{x}) - P_1(\mathbf{x})|/2$, where the sum goes over all possible detection events. In our case, the two distributions are the products of two Poisson distributions and we have numerically observed that their distance is well approximated by $\sqrt{1 - Q}$, where Q is the Chernoff coefficient $Q = \min_{0 \leq s \leq 1} [\sum_{\mathbf{x}} P_0^s(\mathbf{x}) P_1^{1-s}(\mathbf{x})]$, which can be calculated to be $Q = \exp(-\xi n)$, where $\xi = - \min_{0 \leq s \leq 1} [T_0^s T_1^{1-s} + R_0^s R_1^{1-s} - s(T_0 + R_0) - (1-s)(T_1 + R_1)]$. The accessible knowledge is then given by the same expression $f(\xi n)$ as the max-

imum knowledge derived from the Helstrom error bound (but of course with a different ξ), allowing direct comparisons between the two. In our regime of parameters, the minimum is reached for $s \approx 0.5$ leading to $\xi = (T_0 + T_1 + R_0 + R_1)/2 - \sqrt{T_0 T_1} - \sqrt{R_0 R_1} = 0.11$. Taking into account the finite detector efficiencies, the same calculation leads to $\xi = 4.6 \times 10^{-2}$.

Determination of the spontaneous scattering rate The detection light populates the excited state $|F' = 3, m_F = 0\rangle$ which can decay via two channels: spontaneous emission into free space with rate Γ , and into the second orthogonally polarised TEM00 cavity mode which is detuned by 540 MHz [22] with a Purcell-enhanced rate Γ_P (see fig 3). Decay into the original (pumped) cavity mode is not considered since it constitutes a coherent process which does not change the atomic state. The decay into the second cavity mode always leads to a change of the atomic Zeeman state, while for the decay into free space the atom has a probability of 3/5 (given by the transition strengths) to end up in the original Zeeman ground state. Therefore, the total spontaneous emission rate $\Gamma + \Gamma_P$ is higher than the measured decay constant of state $|1\rangle$ (see Fig. 3). To correct for this small effect we have to know the relative probability of the two decay channels. The effect of the second cavity mode is too strong to be treated as a perturbation, therefore we numerically solve the complete master equation (including all ground and excited state Zeeman levels as well as the two cavity modes). From this solution we obtain the ratio of the two decay channels of $\Gamma_P/\Gamma = 2.6$ which only weakly depends on experimental parameters. Using this value we obtain for the spontaneous scattering rate $n/m = \nu^{-1} \times (\Gamma_P + 2\Gamma/5)/(\Gamma_P + \Gamma)$. This ratio is 3.6 times smaller than the value $C/\sqrt{T_0}$ for a single-mode cavity.